ELSEVIER

Ceramics International 28 (2002) 265–270

CERAMICS INTERNATIONAL

www.elsevier.com/locate/ceramint

Effect of magnesium on structure and properties of $LiNbO_3$ prepared from polymeric precursors

A.Z. Simões*, A.H.M. González, A.A. Cavalheiro, M.A. Zaghete, B.D. Stojanovic, J.A. Varela

Chemistry Institute, Physics-Chemistry Department, UNESP C.P. 355, PO Box 14801-970, Araraquara-SP, Brazil

Received 10 April 2001; received in revised form 14 June 2001; accepted 18 September 2001

Abstract

The effect of magnesium addition on the phase formation and electric properties of $LiNbO_3$ powder prepared from polymeric precursor was analyzed. It was shown that the unit-cell volume of the rhombohedral phase decreased with increasing magnesium concentration. Small amounts of secondary phases were observed in $LiNbO_3$ powder doped with 5 and 10 mol% Mg^{+2}. These results indicated that the Mg^{+2} ion was substituted for niobium ion in the rhombohedral phase. The addition of Mg^{+2} promotes densification of $LiNbO_3$ ceramics. It was noticed that the increase in additive concentration leads to a decrease of electric properties, K_p and d_{33}. This is due to formation of $LiNb_3O_8$ and $MgNb_2O_6$ phases at the grain boundaries.

Keywords: A. Calcination; Organic precursors; B. X-ray methods; C. Electrical properties; D. Niobates

1. Introduction

Lithium niobate is well known as an important ferroelectric material. At room temperature, $LiNbO_3$ has a rhombohedral symmetry and space group *R3c*. The ferroelectric-paraelectric transition occurs at about 1200 °C [1]. This material possesses a large number of interesting characteristics such as electro-optic [2] and photo-refractive properties. All these properties make lithium niobate, generally as a single crystal, appropriate for many applications such as optical waveguides [3], frequency doublers [4] and holographic storage systems [5]. However, polycrystalline lithium niobate due to its dielectric properties also has important technological applications [6,7]. Otherwise, those properties are strongly dependent on the method of preparation which determines the final characteristics of the ceramic powders and bulk. It has been demonstrated that the $LiNbO_3$ characteristics could be improved by addition of additives during powder calcination. Recently Mg-doped $LiNbO_3$ has been prepared by conventional procedure by the mixing of oxides (CMO) [8]. In this case Rietveld analysis indicated that the magnesium substitutes for the niobium ion in $LiNbO_3$, showing a great compositional fluctuation. Kanai et al. [9] prepared $LiNbO_3$ by the proton exchange process (PEP) and observed an improvement in the dielectric properties. Fan et al. [8], prepared magnesium doped $LiNbO_3$ by PEP and observed an increase of values for remanent polarization and a decrease of values for coercive field. Fan et al. [10] also observed larger values of remanent polarization and a smaller coercive field for Mg doped $LiNbO_3$ prepared by liquid phase epitaxy (LPE).

By conventional processing [11,12] $LiNbO_3$ was prepared by calcination of a mixture of Li_2O and Nb_2O_5 powders. This process requires a high sintering temperature and causes Li_2O loss. In recent years sol-gel processing [13,14] and the co-precipitation method [15] have become popular for producing ceramic materials with improved compositional homogeneity and lower sintering temperature. Although the sol-gel process utilizes expensive precursors and depends on a critical drying process, the co-precipitation process is limited by cation solutions with similar solubility constants. On the other hand, Pechini's method [16] which employs

* Corresponding author. Tel.: +55-16-201-6600; fax: +55-16-222-7932.

E-mail address: alexsimo@posgrad.iq.unesp.br, biljana@iq.unesp.br or smstobi@yahoo.com (A.Z. Simões).

0272-8842/02/$22.00
PII: S0272-8842(01)00089-X

complexing of cations in an organic media, makes use of low cost precursors and results in a homogeneous ion distribution at the molecular level. Due to the formation of a polyester resin during the synthesis, no segregation of cations was observed during the thermal decomposition of organic material.

Generally, to improve the properties of $LiNbO_3$, the dopants like titanium, zinc and magnesium could be added [17,18]. The addition of small quantities of magnesium produces niobium vacancies (B—vacancy in ABO_3 perovskite) in $LiNbO_3$ and enhances domain reorientation [19], resulting in square hysteresis loop, low coercivity and high remanent polarization. Mg-doped $LiNbO_3$ is used in high-sensitivity devices, such as hydrophones, phonograph pickups, sounders and loudspeakers.

It has been reported that the loss of stoichiometry by Li_2O evaporation during sintering, as well as the formation of niobium-rich grain boundaries decreases the planar coupling coefficient, K_p, and piezoelectric strain coefficient, d_{33}, and affected their reproducibility [20]. Other factors such as defects, grain size, wall domain mobility and density were reported to affect the piezoelectric and dielectric properties [21].

The aim of this work is to study the effect of magnesium addition on $LiNbO_3$ crystal structure and the formation of secondary phases. $LiNbO_3$ (Li/Nb = 50/50) was prepared by using organic citrate solutions with the addition of 1–10 mol% magnesium. To identify the most probable site occupied by the additive in the crystal structure of $LiNbO_3$, and its influence on the formation of non-$LiNbO_3$ crystalline phases, such as $LiNb_3O_8$ and $MgNb_2O_6$, the Rietveld method was applied. Electric properties of the sintered samples were measured to verify the Mg influence on the $LiNbO_3$ electric characteristics.

2. Experimental

The procedure of $LiNbO_3$ synthesis, based on Pechini's method [16], starts from the fact that certain α-hydroxycarboxylic organic acids can form polybasic acid chelates with several cations. After addition of a polyhydroxylic alcohol and heating, the chelate transforms into a polymer, with homogeneously distributed cations. The organic part is subsequently eliminated at temperatures as low as 300 °C, forming reactive oxides with well-controlled stoichiometry. A series of four samples of $LiNbO_3$ were prepared from organic solutions of Li, Nb, and Mg citrates and calcined at 700 °C for 3 h, as follows: (i) without additive, (ii) with 1 mol% magnesium, (iii) with 5 mol% Mg, (iv) with 10 mol% Mg. The additives were added to pure $LiNbO_3$, e.g. 100% $LiNbO_3 + x$% Mg ($x = 1$, 5 and 10).

DTA analyses of resins precalcined at 300 °C for 2 h in a chamber furnace was carried out in a dynamic synthetic air flow (50 cm^3/min) with heating rate of 5 °C/min. TG analyses of resins prepared at 140 °C was carried out in the same conditions described above (SDT2960).

Most of the organic material was decomposed during thermal treatment from room temperature up to 400 °C for 3 h. The formed porous product was crushed and heated in a crucible alumina at 700 °C for 4 h to eliminate residues of organic material. The resulting material was milled in atritor with zirconia balls in an acetone medium for 1 h using the procedure according to [22]. After drying, the powders were isostatically pressed at 230 MPa in pellets 2×12 mm. The pellets were sintered at 1000 °C for 3 h in an open system. The density of the pellets were determined by the water displacement method (Archimedes).

X-ray diffraction data were collected with a Siemens D5000 diffractometer under the following experimental conditions: 40 kV, 30 mA, $5° \leqslant 2\theta \leqslant 70$, $\Delta 2\theta = 0.02°$, λCu K_α monocromatized by a graphite crystal, divergence slit = 2 mm, reception slit = 0.6 mm, step time = 10 s. The Rietveld analysis was performed with the Rietveld refinement program DBWS-941 1 [23]. The profile function used was the modified Thompson–Cox–Hasting pseudo-Voigt, in which η (the Lorentzian fraction of the function) varies with the Gauss and Lorentz components of the full width at half maximum.

3. Results and discussion

In order to determine the best condition of annealing, a thermal analysis were performed. Figs. 1 and 2 show the TG and DTA curves of the pure $LiNbO_3$ and doped with 1, 5 and 10 mol% Mg resins obtained from room temperature up to 1200 °C using a heating rate of 5 °C/min. In these figures the existence of three stages corresponding to the weight and energy change can be observed. The first stage (170–230 °C) is related to elimination of water formed during the process of esterification and excess of ethylene glycol (Fig. 1). In the same temperature range in the DTA curve (Fig. 2) is observed the presence of an endothermic process (170 °C) due to the elimination of water and another small exothermic signal (230 °C) relating to the elimination of solvents. The second one (230 – 500 °C) is associated with the endothermic signal present at 330 °C in the DTA curve and can be related to a break away of the polymeric chains formed by a polyesterification reaction. The third one between 480 and 580 °C is due to the decomposition of organic ligands and crystallization of $LiNbO_3$ phase, which is associated with the very intense exotherm signal observed around the 500 °C in the DTA curve. These results are in agreement with some literature data [24]. Above 1100 °C transformation from rhombohedral to tetragonal phase for pure $LiNbO_3$ occurs. The displacement of temperature above 1100 °C occurred as a consequence of the amount of Mg^{+2} in the doped $LiNbO_3$.

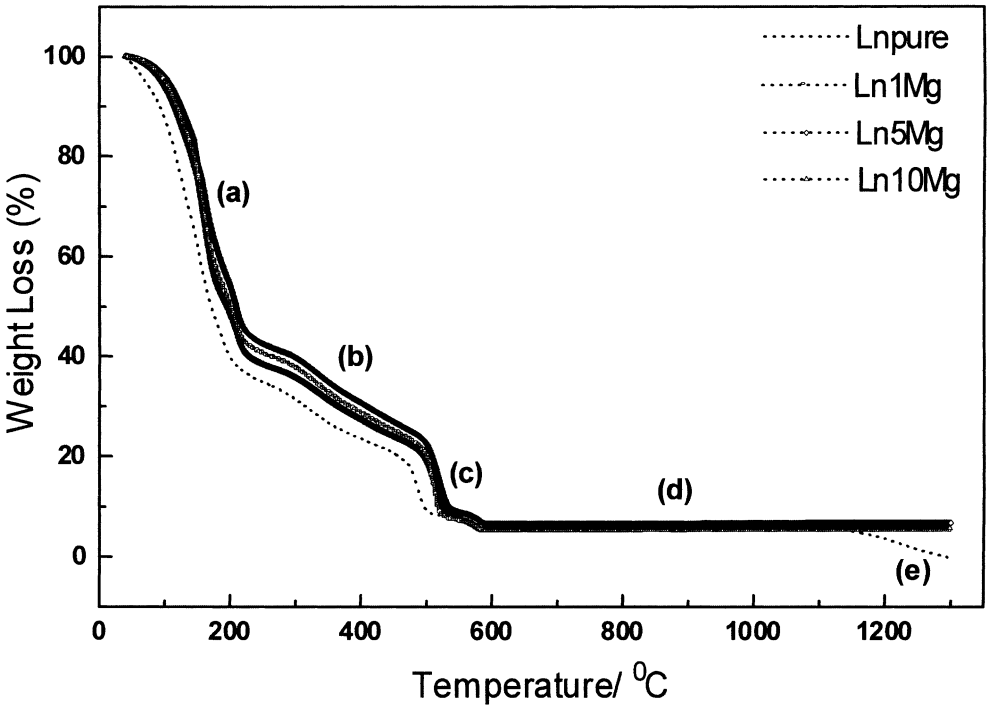

Fig. 1. TG curves of undoped and doped $LiNbO_3$ resin obtained in flow air and heating rate of 5 °C/min.

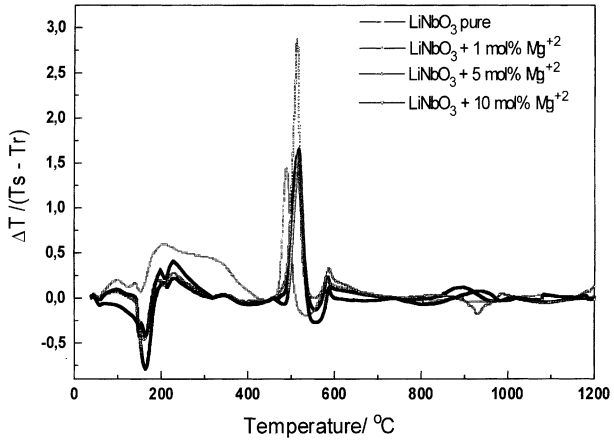

Fig. 2. DTA curves of undoped and doped $LiNbO_3$ resin obtained in flow air and heating rate of 5 °C/min.

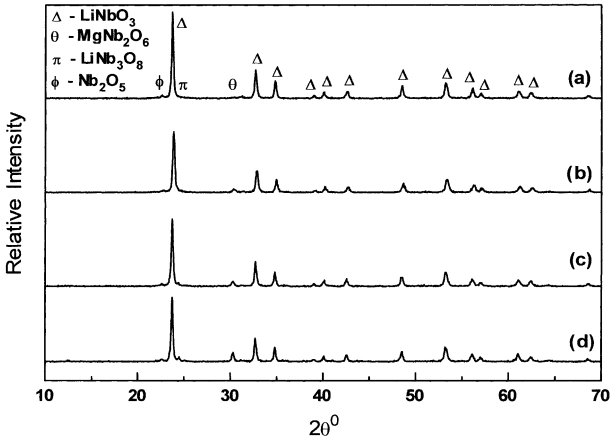

Fig. 3. XRD patterns of doped and pure $LiNbO_3$ powders doped with different concentration of magnesium and calcined at 600 °C for 3 h.

In order to evaluate the effect of the Mg^{+2} addition on the crystal structure of pure $LiNbO_3$, the powders doped with 1, 5 and 10 mol% in Mg^{+2} were calcinated at 600 °C. The X-ray data show the presence of secondary phases Nb_2O_5 at $2\theta = 22.7°$, $MgNb_2O_6$ at $2\theta = 30{,}3°$ and $LiNb_3O_8$ at $2\theta = 24.5°$ (Fig. 3a–d, respectively). It was verified by an increase in the relative intensities of the peaks corresponding to the secondary phases with the increase of the Mg^{+2} concentration. The presence of the Nb_2O_5 phase confirms that the Mg^{+2} ions substitutes for the Nb^{+5} ions in the crystalline lattice producing oxygen vacancies. The reactions of defects formation are presented below:

$$MgO \xrightarrow{LiNbO_3} Mg'''_{Nb} + O_O + 3V_{O^{\cdot}}$$

The quantitative phase analysis of powders as the change of unit cell volume regarding to rhombohedral phase can be observed in Table 1. The Rietveld indexes were calculated according to the reference of Young and Wiles [25]. The obtained results confirmed that Nb^{+5} ion was substituted by magnesium ion in the rhombohedral $LiNbO_3$ phase and no changes occured in the refinements. Contrary, the refinements diverged to absurdly high R_{wp} indexes supposing that Li^{+} ion was substituted by Mg^{+2} ion. The rhombohedral unit-cell volume varied according to the amount of phases

Table 1
Quantitative phase analysis for undoped and doped $LiNbO_3$ samples. Lattice parameters were obtained by Rietveld method

Samples	R_P	R_{WP} (%)	R_{exp}	S	a (Å)	b (Å)	c (Å)	V (Å^3)	Size (Å)	δ (%)
LN pure	8.94	13.22	7.17	1.84	5.1561 (3)	5.1561 (3)	13.8669 (4)	319.26 (3)	4208	0.11
LN1Mg	11.16	15.87	6.85	2.31	5.1555 (4)	5.1555 (4)	13.8663 (4)	319.17 (4)	3430	0.17
LN5Mg	8.08	12.62	6.65	2.02	5.1553 (3)	5.1553 (3)	13.8650 (4)	319.13 (3)	3447	0.09
LN10Mg	7.00	10.76	6.16	1.74	5.1520 (4)	5.1520 (4)	13.8605 (6)	318.61 (4)	1010	0.22

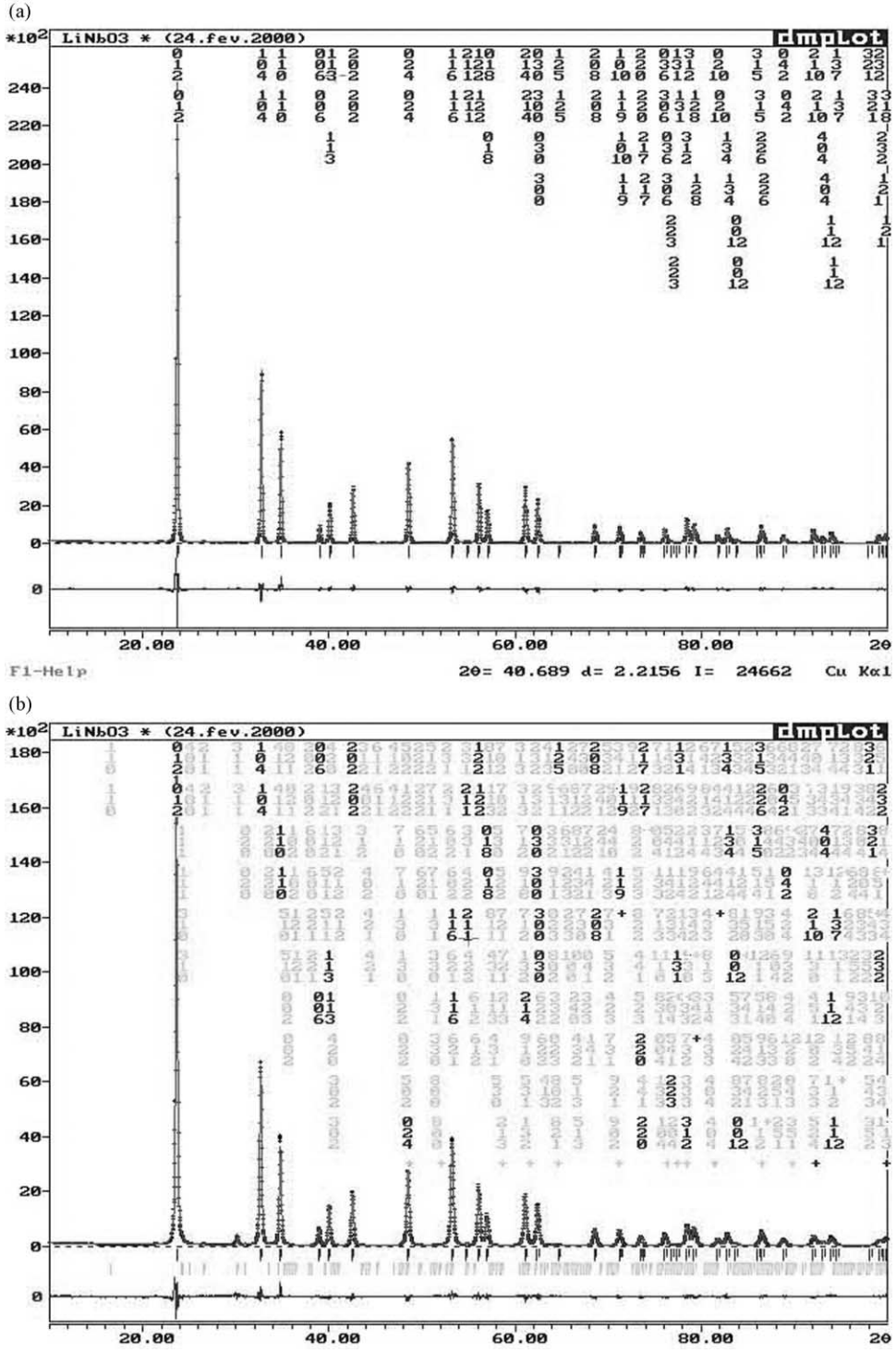

Fig. 4. Rietveld analysis for the $LiNbO_3$ sintered at 1000 °C for 3 h at different magnesium content: (a) 1 mol% Mg^{+2} and (b) 5 mol% Mg^{+2}.

formed and the magnesium addition. The rhombohedral unit-cell volume decreased by increasing the amount of secondary phases. Taking into account that the ionic radius of Nb^{+5} is little higher (0.69 Å) than the ionic radius of Mg^{+2} (0.66 Å), the niobium substitution by magnesium in the rhombohedral unit cell, resulted in the small decrease of unit cell volume. Regarding the values of lattice parameters (a and c) for pure and magnesium-doped $LiNbO_3$, a small decrease with increase of magnesium concentration was observed. Thus, $LiNbO_3$ doped with 10 mol% Mg^{+2} shows the more significant change in the a and c parameters of $LiNbO_3$. This pointed that the limit of solubility of Mg^{+2} in the perovskite lattice is less than 5 mol% of the Mg^{+2}.

Final Rietveld plot for the refinements of the $LiNbO_3$ doped with 1 and 5 mol% in Mg^{+2} is given in Fig. 4a–b. It was observed that the difference between the experimental and theoretical lines is small indicating the good quality of the refinement. For $LiNbO_3$ doped with 5 mol% in Mg^{+2} the difference between the experimental and theoretical lines are evident indicating the presence of secondary phases in investigated system.

It is known that the dopants exert an influence on the properties of $LiNbO_3$ ceramic materials. It can be noticed that Mg^{+2} dopant also has an influence on the reactivity of the powder (Table 2). The addition of dopant decreases the surface area due to the displacement of Nb^{+5} in the crystalline lattice favouring the formation of secondary phases on the surface of the particles during the calcination.

The sintering of $LiNbO_3$ for longer time at temperature above 1000 °C causes weight loss due the lithium oxide volatilization. It can be supposed that during sintering the particles of lithium oxide release a larger amount of vapor reaching the equilibrium pressure on the surface of grains. The evaporation of small particles was caused by gradient of vapor pressure, promoting its permeation through pores. The data of the Table 3 show that the weight loss decreases with the increase of the dopant concentration. Besides that, the green and sintered densities of the pellets doped with Mg^{+2} are higher than the green and sintered densities obtained for the pure $LiNbO_3$. Even so, the relative density decreases with the increase of Mg^{+2} content because of the presence of secondary phases ($LiNb_3O_8$ and $MgNb_2O_6$) with densities of 3.87 and 4.99 g/cm^3. This contributes to lower density of the system.

Table 2
Surface area obtained for $LiNbO_3$ powders calcined at 600 °C for 3 h

Samples	Surface area (m^2/g)
LN pure	17.72
LN1Mg	13.11
LN5Mg	9.96
LN10Mg	8.74

Table 4
Electric and piezoelectric properties of undoped and doped $LiNbO_3$ samples after sintering at 1000 °C for 3 h

Samples	P_r (μC/cm^2)	E_c (kV/cm)	d_{33} (pC/N)	K_p (pC/N)
LN pure	15.4 ± 2%	46.9	2.12	0.39
LN1Mg	13.9 ± 3%	41.9	1.97	0.37
LN5Mg	18.5 ± 2%	63.9	1.79	0.24
LN10Mg	7.3 ± 2%	97.9	0.56	0.12

The data of electric and piezoelectric characterization present the average values of measurement of three samples (Table 4). With increase of dopant concentration, the coercive field is higher resulting in a smaller remanent polarization. This indicates that for 5 and 10 mol% Mg^{+2} the polarization process is more difficult to accomplish, probably due to the presence of $MgNb_2O_6$ which presents a relaxor property and thus inhibits the ferroelectricity of $LiNbO_3$ phase. For both, P_r and E_c, an irregular behavior is observed due to the polarization process which involves the reorientation of the domains. The mechanical deformation, d_{33}, and the electromechanical factor, K_p, decrease with the increase of the dopant concentration because of the presence of secondary phases. The amount of secondary phases influences directly both the d_{33} and K_p values [26]. The presence of these phases affects the stoichiometry, homogeneity and density of doped $LiNbO_3$. The mechanical deformation and the transduce effect have higher values for pure and $LiNbO_3$ doped with 1 mol% Mg^{+2} than for $LiNbO_3$ doped with higher Mg^{+2} content.

4. Conclusions

The obtained results pointed out that:

Table 3
Data obtained for magnesium doped $LiNbO_3$ after sintering at 1000 °C for 3 h

Samples	Weight loss (%)	Green density (g/cm^3)	Sintered density (g/cm^3)	Theoretical density (g/cm^3)	Relative density (%)
LN pure	3.06	2.34	4.01	4.44	90.3
LN1Mg	2.34	2.36	4.04	4.48	90.1
LN5Mg	1.75	2.47	4.12	4.62	89.1
LN10Mg	1.55	2.76	4.21	4.81	87.5

- Magnesium has strong influence on structure and electric properties of $LiNbO_3$.
- The temperature of phase transformation from rhombohedral to tetragonal phase is influenced by the addition of magnesium.
- Mg^{+2} ion substitutes for Nb^{+5} ions in the rhombohedral $LiNbO_3$ phase.
- Addition of more than 5 mol% Mg^{+2} causes the formation of secondary phases such as $MgNb_2O_6$ and $LiNb_3O_8$ which degrade the piezoelectric properties of the $LiNbO_3$.
- Pure $LiNbO_3$ and doped with 1 mol% Mg^{+2} have good potentials for evaluation of their piezoelectric applications.

Acknowledgements

The authors acknowledge FAPESP, CNPq and FINEP/PRONEX, all Brazilian agencies, for financial support to this work.

References

[1] S.C. Abrahams, J.M. Redy, J.L. Bernstein, J. Phys. Chem. Solids 27 (1966) 997.
[2] G.E. Peterson, A.A. Ballman, P.V. Lenzo, P.M. Bridenbaugh, Appl. Phys. Lett. 5 (1964) 62.
[3] I.P. Kaminov, J.R. Carruthers, Appl. Phys. Lett. 22 (1973) 326.
[4] R.K. Tyagi, V.V. Rampal, G.C. Bhar, Infrared Phys. 31 (1991) 319.
[5] P. Gunter, Phys. Rep. 93 (1982) 199.
[6] S.C. Bhatt, B.S. Semwal, Solid State Ionics 23 (1987) 77.
[7] N. Easwaran, C. Balasubramanian, S.A.K. Narayandass, D. Mangalaray, Phys. Status Solidi A 129 (1992) 443.
[8] C.O. Paiva-Santos, M. Cerqueira, E. Longo, J.A. Varela, Y.P. Mascarenhas, Brazilian Ceram. Soc. 2 (1991) 616.
[9] H. Kanai, O. Furukawa, H. Abe, Y. Yamashita, J. Am. Ceram. Soc. 77 (1994) 2620.
[10] T.Y. Fan, A. Cordova-Plaza, M.J.F. Digonnet, R.L. Bayer, H.J. Shaw, Opt. Soc. Am. 3 (1986) 140.
[11] A. Mehta, E.K. Chang, D.M. Smyth, J. Mater. Res. 6 (1991) 988.
[12] D.P. Birnie, J. Am. Ceram. Soc. 74 (1991).
[13] P.K. Gallagher, F. Schrey, Thermochim. Acta 1 (1970) 465.
[14] D.W. Johnson, Ceram. Bull. 60 (1981) 221.
[15] S.I. Hirano, K. Kato, Adv. Ceram. Mater. 2 (1987) 142.
[16] Pechini, M. P. US Patent 3 330 697 (1967).
[17] S. Troiler-McKinstry, R.E. Newnhan, MRS Bull. 28 (1993) 27.
[18] K. Uchino, Problem solving piezoelectric actuators, Morikita, Tokyo, 1991.
[19] H.M. Rietveld, J. Appl. Crystallogr. 2 (1969) 65.
[20] A.H. Webster, T.B. Weston, N.F.H. Bright, Ibid 50 (1987) 490.
[21] S.C. Chiang, M. Nishioka, R.M. Fuerath, J.A. Pask, Ceram. Bull. 60 (1989) 484.
[22] M.A. Zaghete, et al., J. Am. Ceram. Soc. 75 (1995) 225.
[23] R.A. Young, A. Sakthivel, T.S. Moss, C.O. Paiva-Santos, J. Appl. Crystallogr. 28 (1995) 366.
[24] A.Z. Simões, Master thesis, Araraquara Estadual University, Brazil, 1999.
[25] R.A. Young, D.B. Wiles, J. Appl. Crystallogr. 15 (1982) 430.
[26] S.S. Chiang, M. Nishioka, R.M. Fulrath, J.A. Pasdk, Am. Ceram. Soc. Bull. 60 (1981) 484.